Journal of Catalysis 448 (2025) 116195

Contents lists available at ScienceDirect

Journal of Catalysis

journal homepage: www.elsevier.com/locate/jcat

Research article

NMR relaxometry investigation about the role of a protective silica layer on Pd/C catalyst

M. Stucchi [a], A. Engel [b], F. Drault [b], I. Barlocco [a], A. Villa [a], S. Hermans [b], L. Prati [a,*]

[a] Dipartimento di Chimica, Università degli studi di Milano, Via Golgi 19, 20133 Milano, Italy
[b] IMCN Institute, MOST division, Université catholique de Louvain, 1 Place Louis Pasteur, B-1348 Louvain-la-Neuve, Belgium

A B S T R A C T

This work explored the activity and selectivity of Pd nanoparticles (NPs) supported on carbon black (Pd/CB) in the presence of a protective mesoporous silica layer (Pd/CB@SiO_2). The performances of these catalysts were compared for the hydrogenation of benzaldehyde, observing, in addition to the strong stabilizing impact of the presence of silica layer which maintained its activity up to 4 reaction cycles, differences in the reaction kinetic, particularly concerning product formation and selectivity. Indeed, besides its proper function of protecting Pd NPs, the porous layer of SiO_2 could influence the catalyst-reactant interaction, which in turn modifies the selectivity of the reaction. Therefore, in parallel to the conventional analysis of the catalytic experimental data, the effect of the presence of the silica layer has been studied by NMR relaxometry, as a non-conventional approach of interface characterization operating in the presence of solvent. Considering the hydrogenation of benzaldehyde to benzyl alcohol and toluene, the presence of the SiO_2 layer did not influence the activity of the catalyst in terms of reaction rate, but it changed the formation of the products. NMR analyses disclosed the reason on the basis of such difference, showing that the silica layer tends to increase the interaction of the aromatic ring with the catalyst surface, thereby controlling how the molecule approaches the surface of the catalyst active sites.

1. Introduction

Supported metal nanoparticles have always attracted attention as active and selective catalysts for several reactions of industrial interest [1]. Among them, hydrogenations are of primary importance being fundamental reactions in various processes, including the hydrogenation of the carbonyl bond of aldehydes into the corresponding alcohols. Pd supported on carbon catalyst (Pd/CB) is one of the best-known catalysts for hydrogenation reactions in both gas and liquid phases, due to its capacity to dissociate and easily activate molecular hydrogen [2–4]. However, especially considering liquid phase reactions, one of the main drawbacks of small metallic particles as active phase is the catalyst stability, as well as the risk of leaching and sintering, which causes a fast loss of activity [5]. This is particularly true in the field of hydrogenation/hydrogenolysis reactions, where, in addition to the presence of palladium as a hydrogen activator, its protection is crucial to maintain the catalyst stable as possible, being the reaction conditions usually harsh, both in terms of pressure and temperature.

Therefore, different strategies have been exploited for prolonging the catalyst life, such as the encapsulation of metal nanoparticles (yolk shell configuration) in porous oxide materials, in ZrO_2 or SiO_2 for instance, which can strongly reduce the deactivation by sintering [6,7], even at high temperatures. Among them, some carbon-supported Pd nanoparticles coated with a well-structured mesoporous silica layer anchored covalently onto the carbonaceous surface (Pd/CB@SiO_2) are particularly interesting [8]. These materials have in fact proven to be very promising in the field of hydrogenation reactions. The protection of Pd NPs was indeed demonstrated to be crucial to maintain the catalyst stable for several catalytic cycles, with particular emphasis when harsh reaction conditions, in terms of pressure and temperature, are required, which is usual in the field of hydrogenation/hydrogenolysis reactions.

Beyond the experimentally proved improvement of the stability of the Pd NPs protected with mesoporous silica (Pd/CB@SiO_2), observable from the catalytic data [8], there is the possibility to get additional information about the intrinsic role of the SiO_2 layer on the catalyst-reactant interaction, under conditions that reproduce the catalytic system. In this way, there would be the prospect to disclose how the catalytic surface and its morphological features can interfere in the interaction of the different catalytic subjects (substrates, solvent), thus considering the whole catalytic system.

The study of the whole catalytic behaviour as a result of a complex interplay between the catalyst structural properties, reactants and reaction medium, where the adsorption/desorption of reactants and products plays a crucial role, is therefore the key concept based on this research [9].

The study of the phenomena that play some roles in the catalytic

* Corresponding author.
E-mail address: laura.prati@unimi.it (L. Prati).

https://doi.org/10.1016/j.jcat.2025.116195
Received 5 March 2025; Received in revised form 28 April 2025; Accepted 30 April 2025
Available online 6 May 2025

activity of a certain material, in a certain reaction, is usually carried out through microscopic and spectroscopic techniques, like High-resolution transmission electron microscopy (HR-TEM), X-ray photoelectron spectroscopy (XPS), and Fourier-transform infrared spectroscopy (FT-IR), which give mostly information about the catalytic material, for example about metal NPs dispersion, their dimensions, surface exposure, oxidation state and interaction with the support, which globally can be related to the final catalytic performance[10]. By FT-IR spectroscopy of probe molecules [11] it is possible to investigate substrate adsorption on catalytic support [12] but in the case of a heterogeneous catalytic system in liquid phase, the possible influence of the solvent would be completely disregarded. Another option then could be to perform experiments by Attenuated Total Reflection spectroscopy (ATR-IR), where for example CO adsorption on different solid catalysts can be investigated in the presence of gas or water [13], or also it can be studied the interaction between an organic liquid substrate (i.e., benzyl alcohol in cyclohexane) on a metal-based catalyst (like Pd NPs supported on Al_2O_3) revealing important information about the metal active sites [14], but unfortunately this technique does not apply to carbons.

Another possible approach is the comparison between reactant heat adsorption values, but in liquid phase such measurements are not very reliable if the final aim is to correlate the catalytic activity with the whole system because of the presence of the solvent. In our previous studies [4,15,16] we demonstrated that measurements based on NMR relaxometry could be more representative for explaining the catalytic activity in liquid phase.

Nuclear Magnetic Resonance spectroscopy (NMR) can be used as unconventional technique to investigate the interaction of reactants and catalytic solid materials in the presence of the solvent [15]. More precisely, the NMR spin relaxation can be studied as a sensitive probe for molecular dynamics [16]. In fact, relaxation times (the longitudinal T1, and the transverse T2) depend on the rotational correlation time of a reactant [17] and may be used to identify molecular dynamics processes. What is particularly interesting to be associated with the study of heterogeneous catalytic systems is that reduced T1 and T2 relaxation times are observed when liquid molecules interact with a solid surface, because of a decrease in molecular mobility [18].

NMR relaxometry calculations are based on the principle that, after excitation by a radiofrequency wave, nuclei in a magnetic field produce a decaying signal, exchanging energy with the environment and also with the catalyst surface, upon interaction. In this way, the study of Nuclear Magnetic Resonance (NMR) signal decay or relaxation (relaxometry) can give insight into the dynamics and interactions of the molecules with the catalyst surface, which is a crucial factor in determining the final catalytic behaviour.

We have already developed a protocol based on T1 ^{13}C NMR to be used to study some heterogeneous catalytic systems where carbon-based catalysts were adopted [15]. The great advantage of this method was the possibility to discriminate the individual resonances of each single carbon atom of the organic substrate, due to the larger chemical shift range of ^{13}C [19]. Moreover, the T1 longitudinal relaxation time was used by its own, avoiding some issues related to the use of T2 in this kind of systems, as detailed in the next paragraphs.

1.1. T1 or longitudinal relaxation

An excitation pulse acts to disturb a spin system from its thermal equilibrium. After a given time, equilibrium is restored *via* spin–lattice or longitudinal relaxation with an exchange of energy with the 'lattice'. The thermal equilibrium is restored following an exponential behaviour according to Bloch theory [20]. The return of the longitudinal magnetisation (M_z) after a perturbation, with T_1 as the first-order time constant, along the static field B_0, can be described by equation (1):

$$\frac{dM_Z}{dt} = -\frac{M_Z - M_0}{T_1} \tag{1}$$

where M_0 is the equilibrium magnetisation.

Considering $M_z(0)$ the longitudinal magnetisation at t = 0, it can be obtained the equation (2):

$$M_Z = M_Z(0)\exp(-t/T_1) + M_0(1 - \exp(-t/T_1)) \tag{2}$$

$M_z(0)$ is equal to zero after a 90° pulse, and thermal equilibrium is fully re-established at time $t = 5xT_1$. Different pulse sequences can be applied to obtain the T_1 value. In this work, the T1 measurements were obtained using a standard inversion recovery. The inversion-recovery pulse sequence consists on an initial 180° pulse to invert the equilibrium magnetization and align it along –z. The magnetisation recovers towards thermal equilibrium during a time τ_R following an exponential function (eq. (2)). A 90° pulse is applied to determine the value of the magnetisation vector. Then, the use of different recovery times (τ_R) would yield different M_z values to be fitted into the equation (3), to finally obtain T_1:

$$M_Z = M_0(1 - 2\exp(-\tau_R/T_1)) \tag{3}$$

1.2. The use and explanation of the ^{13}C $T1_{ads}/T1_{bulk}$ ratio

Overall, reduced T1 and T2 relaxation times are observed when liquid molecules have an interaction with a solid surface due to a change in the molecular mobility [18]. In bulk liquids, T1 = T2. Upon adsorption, enhanced surface interactions will occur for both T1 and T2. But, T2 is more influenced than T1 by translational and rotational dynamics, making reliable the use of the ratio of relaxation times T1/T2 to compare interactions of different liquid substrates and materials. In this sense, the relaxation time ratio is a qualitative indicator of surface interaction strength, where an increase in the surface interaction will result in an increase of the T1/T2 ratio. However, there are some problems related to the use of T2 in these kinds of systems: T2 can be influenced by molecular diffusion in magnetic field gradients, that can be particularly significant in studies of porous materials (where any contrast in magnetic susceptibility between the adsorbent and the adsorbate will induce a perturbation in the uniform field). Moreover, such perturbation is more pronounced at high magnetic fields, such as the one used in this work (400 MHz). On the contrary, the T1 relaxation times are independent of such artefacts that preclude an accurate interpretation of T1/T2 results [21]. To overcome this issue, T1 can be used without the T2.

The molecular motion of the adsorbate of the adsorbate on the surface of the adsorbent is described by the autocorrelation function $G(\tau)$ averaged over the time interval τ. The Fourier-transform of this function is proportional to the longitudinal relaxation time T_1. The autocorrelation function of the molecule will change on adsorption, manifested in a change in $T1$ [22]. The more energetically stable adsorption conformations can be related to a reduced mobility of the surface-bond species, resulting in a decrease of the T1 in the presence of a surface (if there is interaction) compared to that of the pure bulk molecule. Therefore, the ratio of $T1$ relaxation times for surface adsorbed (ads) to free diffusing (bulk) molecules ($T1_{ads}/T1_{bulk}$) can be used as an indicator of the relative strength of surface interaction. A low $T1_{ads}/T1_{bulk}$ ratio is thus associated with low mobility and stronger interaction. The only boundary condition to consider is that the results can be related only to the adsorption/interaction of a monolayer, so that the geometric effects of the pore are not relevant and it will be possible to compare the relaxation time of the adsorbed liquid molecules to those in the bulk as an indicator for different adsorbate-adsorbent pairs. At this point, the advantages of the use of the $T1_{ads}/T1_{bulk}$ ratio for heterogeneous catalytic materials can be clearer.

1.3. Application to the methodology to Pd/CB and Pd/CB@SiO_2 catalysts

The use of nuclear magnetic resonance (NMR) relaxation as a tool for characterizing porous media is quite well-established [23]. Applications related to diffusion in nanopores, fluids in petroleum deposits and gas

adsorption in nanoporous media are exciting areas of recent development. Our previous approaches concerned, as described before, the use of high-filed (400 MHz) especially for carbon-based materials [15,24]. In addition, this method has been already used to investigate oligomers grafted onto silica surfaces [25], surfactants adsorbed on silica [26], and within catalysis, for example to study the adsorption of hydrocarbons on zeolites [27].

From here, the purpose of this research is to apply the principle to study the benzaldehyde hydrogenation by these catalytic materials, which is made up of a mesoporous silica layer specially built on Pd NPs supported on carbon, leaving free access to the active sites thanks to its porosity. Considering the rather high complexity of the system, learning about the impact of the catalyst morphology and structure on the whole molecular dynamics in a liquid-phase catalytic system, will be beneficial to understand how to control it.

As described previously, the ratio of T1 relaxation times for surface adsorbed (ads) to free diffusing (bulk) benzaldehyde has been used as an indicator of the relative strength of interaction of each C atom of the substrate with the catalyst surface. Accordingly, some considerations about the plausible molecule approach to the catalyst surface can be done.

So, the improvement obtained by modifying Pd supported on carbon (Pd/CB) by silica (Pd/CB@SiO_2) [8], here is investigated by comparing their catalytic behaviour using benzaldehyde as a model organic substrate, but through two parallel but interconnected channels, i.e., collecting data by conventional catalytic tests and by unconventional NMR experiments.

Through conventional catalytic experiments, we classically explored the activity and selectivity of Pd/CB@SiO_2-protected catalyst vs the non-protected Pd/CB. In this context, the differences between Pd/CB and Pd/CB@SiO_2 were obtained by a mere collection of the catalytic results. In parallel, the effect of the presence of the silica layer on the interaction of reactants with the catalyst surface has been investigated, as detailed before, by high-field ^{13}C NMR relaxometry [3]. In particular, the correlation of NMR results together with the catalytic performance allows a detailed understanding of the materials features and peculiarities.

1.4. Benzaldehyde hydrogenation: Some considerations about the reaction pathway

The reaction pathway associated with benzaldehyde hydrogenation (Scheme. 1) comprises the direct hydrogenation of the carbonyl functional group forming benzyl alcohol (1). Benzyl alcohol can be further hydrogenated to cyclohexylmethanol through aromatic ring hydrogenation (2), or it can undergo hydrogenolysis to toluene (3), or even it can be transformed to benzene through the cleavage of the C–C bond (4). Toluene or benzene could be also formed directly from benzaldehyde (5–6) [28].

According with the Scheme 1, the formation of toluene or benzene could be consecutive or parallel to benzyl alcohol formation, while the eventual formation of cyclohexylmethanol is always after benzyl alcohol further hydrogenation.

In this work, the morphological differences of the catalysts, due to the presence of the SiO_2 mesoporous layer on Pd nanoparticles, played a role on the products formation during benzaldehyde hydrogenation, forming benzyl alcohol and toluene with different rates. This behaviour has been clarified by studying the interaction of both reactant and products by NMR relaxometry, for the first time.

2. Experimental

2.1. Catalysts synthesis

The reference catalyst consisting of Pd nanoparticles (NPs) supported on carbon black (CB) has been synthesized by a classical precipitation-reduction (PR) method [29]. The chosen support, a commercial CB, was purchased from IMERYS GRAPHITE & CARBON (S_{BET} (m^2/g) 63; Vp (cm^3/g) 0.14). All the reagents, i.e. sodium carbonate (Na_2CO_3), sodium borohydride ($NaBH_4$, >98 %) and sodium tetrachloropalladate(II) (Na_2PdCl_4, 98 %), were purchased from Sigma Aldrich and used as received. For the synthesis, 1 g of CB was dispersed in 100 ml of a Na_2CO_3 2.5 wt% aqueous solution. While maintaining the suspension under stirring, an aqueous solution of 56 mg of Na_2PdCl_4 in 20 ml of distilled water was added dropwise over 1 h, to achieve a theoretical loading of 2 wt% Pd. Then, 5 g of $NaBH_4$ was dissolved in 20 mL of distilled water and added to the CB/Pd salt suspension. After 2 h of

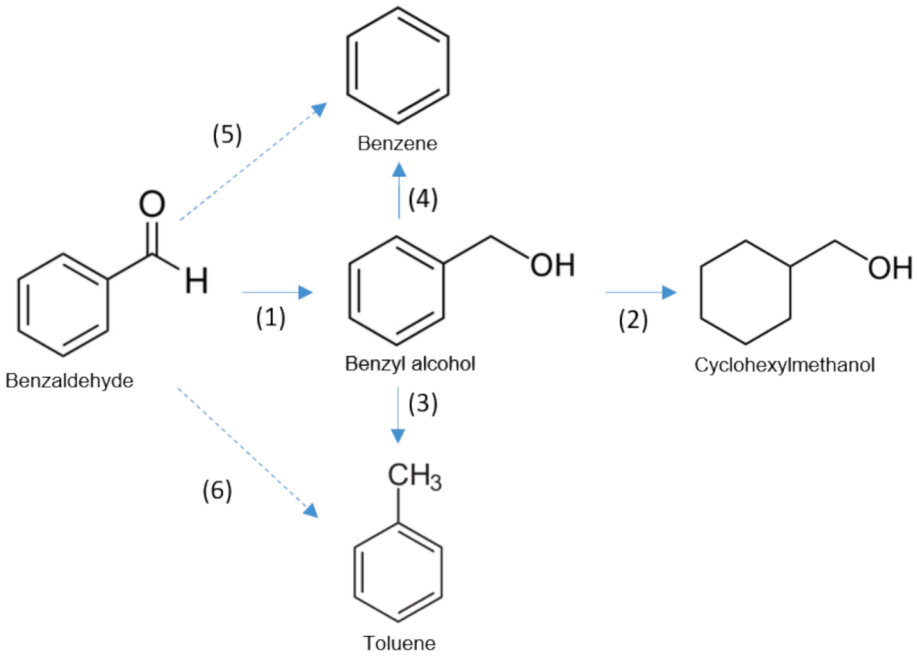

Scheme 1. Reaction pathway associated with benzaldehyde hydrogenation.

stirring, the reduced NPs catalyst (Pd/CB) was filtered, washed with 1 L of distilled water and dried overnight at 100 °C.

The synthesis of the coated Pd/CB@SiO_2 catalyst was performed in 3 steps. Firstly, the CB-APTES material was prepared, using thionyl chloride ($SOCl_2$,>99 %) and (3-aminopropyl)triethoxysilane (APTES, 99 %) as reagents (Sigma Aldrich). For this preparation, 2 g of CB was added to a round-bottom flask containing 100 ml of toluene, where 6 ml of $SOCl_2$ were added. This solution was heated at 120 °C for 5 h under reflux, then filtered and extensively washed with toluene. The resulting material (CB-Cl) was dried overnight under vacuum at 100 °C. 1 g of CB-Cl was then introduced in a round-bottom flask containing 100 mL of dichloromethane and 1 mL of APTES. This solution was stirred for 24 h at room temperature, yielding the amine-grafted material (CB-APTES), which was filtered, washed with dichloromethane and methanol and dried overnight under vacuum at 100 °C. In the second step, using the pre-synthesized CB-APTES as support, a Pd/CB-APTES catalyst was prepared using the same synthesis conditions as the reference catalyst described above. In this case, a nominal loading of 2.5 wt% Pd was used to balance the dilution effects of the covering layer. In the third and last step, the Pd/CB@SiO_2 catalyst was synthesised starting from 0.25 g of Pd/CB-APTES. In a 100 mL round bottom flask containing 25 mL of distilled water and the set amount of Pd/CB-APTES, 10 mL of NaOH (0.1 M) were added and the suspension was sonicated for 10 min. 0.571 g of hexadecyltrimethylammonium bromide (CTAB, >98 %) was added to this suspension and the solution was heated at 60 °C. 0.7 mL of tetraethyl orthosilicate (TEOS, >98 %) was then added dropwise within 30 min. This suspension was further stirred for 3 h, then charged into a propylene bottle, which was closed tightly and heated at 100 °C for 3 days. The solid product was filtered out, washed with ethanol (250 mL) and dried at 100 °C overnight. The CTAB template was removed by refluxing the solid material (Pd/CB@SiO_2) in a 250 mL ethanol/methanol (1:1) mixture for 24 h. Schematic flowcharts of each step have been reported in Fig. S10 in the SI.

2.2. Characterisation techniques

The Pd/CB and Pd/CB@SiO_2 materials, including the bare supports, were previously fully characterized [8] by X-ray photoelectron spectroscopy (XPS), transmission electron microscopy (TEM), elemental analyses (ICP) and N_2 physisorption.

XPS analyses were carried out with an SSI-Xprobe (SSX 100/206) photoelectron spectrometer from Surface Science Instruments (USA), equipped with a monochromatized microfocus Al Xray source. Samples were affixed to small sample holders with double-sided adhesive tape and then placed onto an insulating ceramic carousel (Macor®, Switzerland). Charge effects were avoided by placing a nickel grid above the samples and using a flood gun set at 8 eV. Binding energies were calculated with respect to the C-(C, H) component of the C1s peak fixed at 284.8 eV. Data analysis was performed using the CasaXPS program (Casa Software Ltd., UK).

TEM images were obtained using a LEO 922 Omega Energy Filter Transmission Electron Microscope operating at 120 kV. The samples were suspended in hexane under ultrasonic treatment and deposited onto a holey carbon film supported on a copper grid (Holey Carbon Film 300 Mesh Cu, Electron Microscopy Sciences), and dried overnight under vacuum at room temperature.

Measurements of the nitrogen adsorption–desorption isotherms were achieved by using a Micromeritics ASAP 2020 analyzer at 77 K. Samples were degassed for 2 h at 473 K with a heating rate of 10 K/min under 0.133 Pa pressure. Specific surface areas (SSA) were calculated with the Brunauer–Emmett–Teller (BET) equation. The pore volume (Vp) of the samples and the average pore diameter were calculated using the Barrett-Joyner-Halenda (BJH) model.

Elemental analyses (C, H, N, O) were performed by MEDAC Ltd., (UK) using microgravimetry for C, H, N, O (direct measurement).

ICP analyses were performed by an Optima 8000 Perkin-Elmer instrument. Samples digestion has been performed in 2 steps, the first using a mixture of HNO_3 (36 %) and H_2O_2 (30 %) in ratio 1:2 together with 100 µl of HF (47–51 %), then the second by adding HNO_3 (36 %).

2.3. Catalytic tests

Catalytic reactions were carried out in a 125 mL stainless steel high-pressure autoclave (PressureSyn, High safety reactor, Asynt). In a typical experiment, 15 mL of the substrate solution (benzaldehyde 0.3 M in p-xylene or octanal 0.15 M in dodecane) and an appropriate amount of catalyst to achieve a Pd:substrate molar ratio of 1:1000 were placed in the reactor with a magnetic stirrer. The autoclave was first flushed with N_2 to remove any residual oxygen from the atmosphere, then pressurized to the desired H_2 pressure and heated up to the desired temperature. Sampling was carried out by stopping the stirring, quenching the reaction under cold water, and separating the catalyst from the reaction solution by centrifugation. 1-dodecanol was used as an external standard for GC measurement. Product analysis and quantification were carried out using a GC-FID equipped with a nonpolar column (Thermo Scientific, TRACE 1300 equipped with an Agilent HP-5 column).

The initial activity, expressed in h^{-1}, was calculated after 15 min of reaction as Eq. (4),

$$\frac{Substratemols_{initial} * conv.\%_{at\ 15'}}{molmetal * time(h)} \quad (4)$$

where mol of substrate converted is defined as difference between initial moles and moles detected by GC.

2.4. NMR analyses

p-Xylene-d_{10} was purchased from Sigma-Aldrich and used as a reference solvent. The experiments have been performed also using non-deuterated *p*-xylene, obtaining comparable T1 values, but reducing the resolution of the NMR spectra signal. For this reason, results reported in the following paragraphs derived from the analyses performed by *p*-Xylene-d_{10}. This is the best protocol to follow. The NMR tube was prepared by adding the catalyst and the solution of the various substrates in p-xylene-d_{10}, calculating the proper amount of the liquid to have the complete filling on the pores. The concentration of the substrate solution was set considering that used in the catalytic experiments. NMR analyses were carried out on a Bruker Avance NEO 400 MHz spectrometer at 298 K.

For compound characterisation and ^{13}C chemical shift identification, the J-modulated spin-echo sequence was used with 64 k points in the time domain and 256 scans. T1 measurements were obtained using standard inversion recovery from Bruker library (T1 measurements using inversion recovery with power gated decoupling), following the assumptions described in the introduction.

One is that the equilibrium is approached exponentially, thus the magnetisation along the *z*-axis is represented by Equation (5),

$$M_z = M_0\left(1 - e^{-t/T1}\right) \quad (5)$$

where M_0 is the magnetization at thermal equilibrium, t is the time elapsed, and T1 is the time constant that is obtained by plotting M_z as a function of time. The pulse sequence used in the inversion-recovery experiment is shown below (Eq. (6)):

$$d1 - p1(180^\circ) - d2 - p2(90^\circ) - FID \quad (6)$$

In this experiment, the nuclei are first allowed to relax to equilibrium. A 180° pulse (p1) is then applied to invert the signals. The signals are then allowed to relax for a length of time (d2) that is varied in each experiment. After the variable d2 (recovery delay), a 90° pulse (p2) was applied, and the FID was recorded. The FID records the spectrum intensity as a function of the variable delay d2. The signal will have

relaxed more with longer d2. The peak intensity will reflect the extent to which each signal has relaxed during the d2 period.

^{14}T1 recovery delays were used ranging from 0.05 ms to 100 s. We used 8 repeat scans and a relaxation delay (d1) of 50 s between each scan to ensure a maximum signal (and to ensure the reach of the equilibrium, the d1 delay in the pulse sequence should be set to ~ 5 × the longest T1 of interest in the molecule) was maintained at all times.

The analysis of the T1 measurements was performed with the standard Bruker routine for T1/T2 calculation and with the Bruker Dynamic Centre software version 2.7.1, using the following fitted function (Eq. (7)):

$$f(t) = Io \times [1 - a \times exp(-t/T1)] \quad (7)$$

where I_0 is the equilibrium magnetization and the parameter a determine the magnetization at time zero, that thus corresponds to $I_0(1 - a)$. The errors associated with fitting the bulk and adsorbed T1 were all within ± 1 %.

3. Results and discussion

3.1. Catalysts characterization

The synthesis of the silica-protected Pd/CB catalyst has been optimized previously and it was fully characterized. Previously reported TEM images [8] clearly showed the presence of a silica layer uniformly deposited on the catalyst surface in the sample named Pd/CB@SiO_2, as compared to the bare Pd/CB catalyst (Fig. 1a and c and Figs. S8 and S9 in SI). Further 3D electron microscopy analysis [8] also showed that the silica covered both C and Pd NPs, with mesopores clearly observed above the Pd NPs positions, confirming the mesoporous character of the entire silica shell. This is crucial to maintain an optimal accessibility to the underlying Pd active phase. The formation of a porous layer surrounding the catalyst was also confirmed by nitrogen physisorption measurements, which showed a specific surface area of 56 and 402 m^2/g for Pd/CB-APTES and Pd/CB@SiO_2, respectively. The same trend is observed for pore volume, with 0.19 cm^3/g and 0.36 cm^3/g measured for Pd/CB-APTES and Pd/CB@SiO_2, respectively. XRD analyses provided information about the mesoporous phase, which was identified as MCM-type, more precisely as a mix of MCM-41 and MCM-48, which is ideal for having a 3D network of pores in the layer.

The Pd loadings were determined by ICP analyses, revealing values of 2.97 ± 0.05 % wt. and 1.49 ± 0.05 % wt. for the Pd/CB and Pd/CB@SiO_2 catalysts, respectively. These values were taken into account to perform the catalytic tests by engaging the same metal/substrate ratio, allowing to properly calculate the initial activity. Pd particle size revealed by TEM analyses resulted in average particle sizes of 3.8 ± 1.1 nm and 4.5 ± 1.1 nm for the Pd/CB and Pd/CB@SiO_2 catalysts, respectively.

3.2. Catalytic tests

The activity of the reference Pd/CB compared with that of the modified Pd/CB@SiO_2 catalyst has been investigated for benzaldehyde hydrogenation (Fig. 2). As preliminary test, also the bare CB and CB@SiO_2 supports have been tested showing negligible activity (See SI and Fig. S7).

The activity of Pd-supported on carbon catalysts in this reaction is well known [30], therefore it was used to highlight any possible differences, with particular attention to the reaction pathway (see also scheme 1).

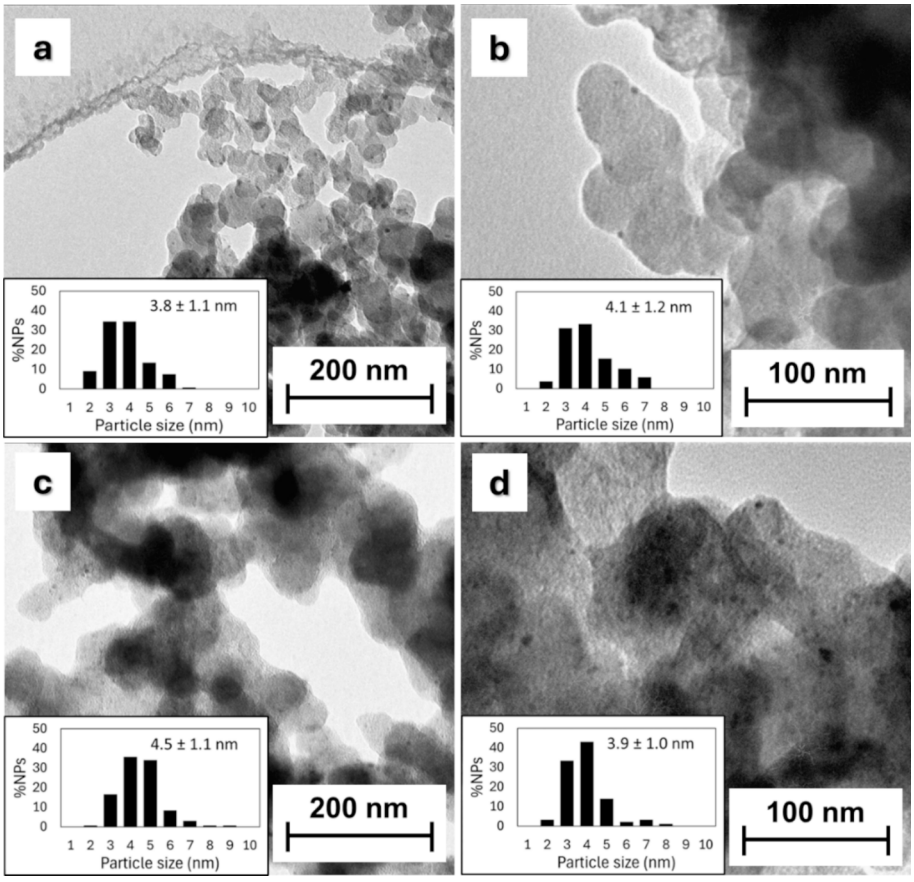

Fig. 1. TEM micrographs of Pd/CB (a fresh and b used), Pd/CB@SiO_2 (c fresh and d used), before and after four recycling, respectively (benzaldehyde hydrogenation, 50 °C and 2 bar H_2). The insets are the histograms of the Pd particle size distributions measured on the TEM images.

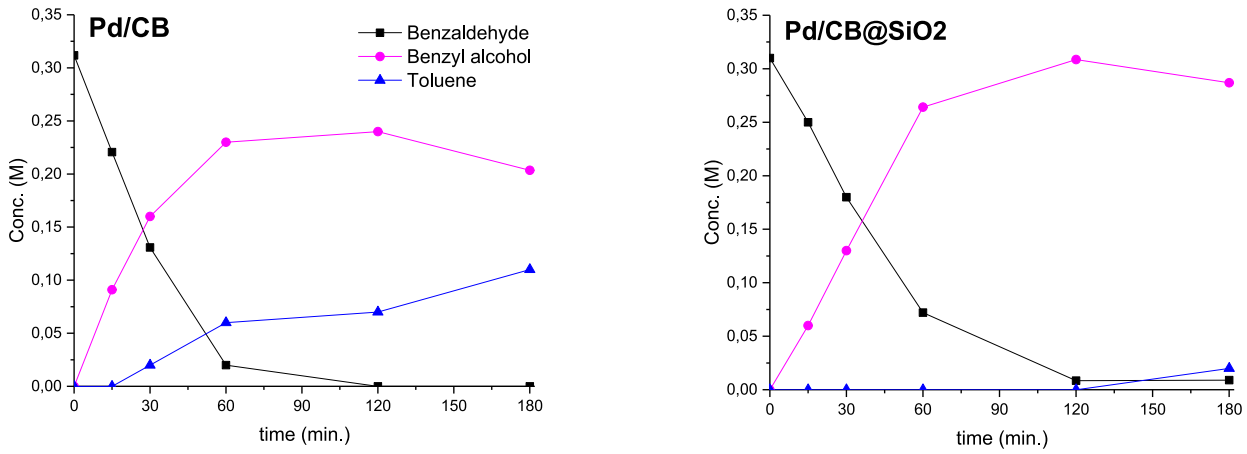

Fig. 2. Evolution of the reaction composition during the benzaldehyde hydrogenation using Pd/CB (left) and Pd/CB@SiO_2 (right) as catalysts. Reaction conditions: benzaldehyde 0.3 M in p-xylene, 50 °C, 2 bar H_2, metal/substrate 1:1000.

Both catalysts were active with high rates of benzyl alcohol formation (Fig. 2, pink lines), but showed different initial activities, of 1249.8 h^{-1} in the case of Pd/CB and 750.2 h^{-1} in the case of Pd/CB@SiO_2. This is not surprising figuring out a slower rate for the catalyst with a larger particle size and a covering layer which possibly shields active sites. However, the two catalysts also showed a marked difference in toluene formation rate (Fig. 1, blue line with triangles), where the non-protected Pd/CB formed toluene straight from the beginning of the reaction, whereas the protected catalyst converted a small amount of benzyl alcohol to toluene only at the end of the reaction window explored.

To determine if the toluene formation by the protected Pd/CB@SiO_2 catalyst was simply slower than that obtained with Pd/CB, the reaction was continued for up to 6 h (Fig. 3), demonstrating the activity of the Pd/CB@SiO_2 catalyst towards hydrogenolysis as well.

It should be noted that the slower reaction rate obtained with the Pd/CB@SiO_2 material can be considered as advantageous for achieving more selective catalysis either for hydrogenation or for hydrogenolysis. Indeed, benzyl alcohol can be obtained with 100 % selectivity after 1 h of reaction, with approximately 75 % conversion of benzaldehyde, or the reaction can be extended to target toluene formation.

In addition, for testing the impact of the presence of water produced in the reaction on Pd/CB@SiO_2 activity and considering the scarce solubility of water into p-xylene, we performed a test saturating p-xylene with water. We did not see any relevant differences in term of both activity or selectivity of the reaction. To be noted that the same catalysts was previously used in water for the oxidation of glucose to gluconic acid [29].

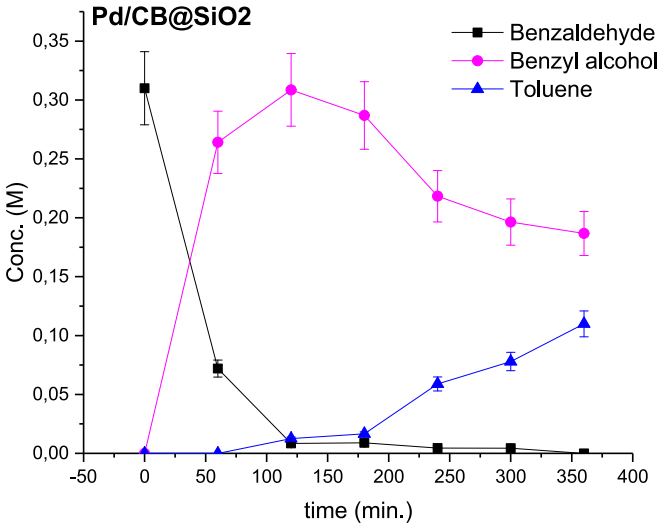

Fig. 3. Benzaldehyde hydrogenation with Pd/CB@SiO_2 catalyst, with reaction time extended to 6 h. Reaction conditions: benzaldehyde 0.3 M in p-xylene, 50 °C, 2 bar H_2, metal/substrate 1:1000.

Another advantage of having protected the active phase Pd NPs is its potential to enhance catalyst durability and reusability. Therefore, recyclability tests were performed on both Pd/CB and Pd/CB@SiO_2 catalysts for reactions of 3 h each (Fig. 4).

The difference between the two catalysts became evident immediately from the second run. The activity of the non-protected Pd/CB catalyst decreased dramatically, losing almost 50 % of its activity within the 4th run. In contrast, the Pd/CB@SiO_2 catalyst showed a slight increase in the activity in the 2nd run followed by sustained initial activity.

Considering that the Pd/CB@SiO_2 catalyst reached almost full benzaldehyde conversion after 3 h of reaction, additional recycling tests on 1 h reaction have been performed (Fig. S11). In this latter case the benzaldehyde conversion was about 76 % after the 1st run and the same conversion was maintained for the next 3 recycling tests, confirming also in this case the stability of this catalyst.

The origin of the activity loss was investigated by comparing fresh and used catalysts in terms of Pd loading and NPs sizes. The ICP analyses of the spent catalysts showed that the Pd loading decreased to 1.52 ± 0.05 % for the uncovered Pd/CB catalyst compared to the initial 2.97 ± 0.05 %, while for Pd/CB@SiO_2, the loading of 1.31 ± 0.05 % after 4 runs was only slightly decreased compared to that before reaction (1.49 ± 0.05 %).

Used catalysts were also characterized by TEM (Fig. 1b and d) to evaluate the size and distribution of Pd NPs before and after tests.

The reference catalyst (Pd/CB) presented particle size of 3.8 ± 1.1 nm before use (Fig. 1a), which slightly increased to 4.1 ± 1.2 nm after the benzaldehyde hydrogenation catalytic test (Fig. 1b). This phenomenon is explained by sintering of Pd as well as leaching/redeposition mechanism. The fresh counterpart protected catalyst (Pd/CB@SiO_2) prior catalytic test presented a larger particle size of 4.5 ± 1.1 nm (Fig. 1c). The used catalyst presented a slight diminution of particle sizes down to 3.9 ± 1.1 nm (Fig. 1d), may due to the presence of hydrogen during the reaction that can reduce the oxidized overlayer produced during silica coating. This finding could explain the slight increase of activity shown after the first run (Fig. 4).

3.3. NMR adsorption analyses

The comparison of Pd/CB and Pd/CB@SiO_2 behaviours in the catalytic hydrogenation of benzaldehyde showed that the SiO_2 layer

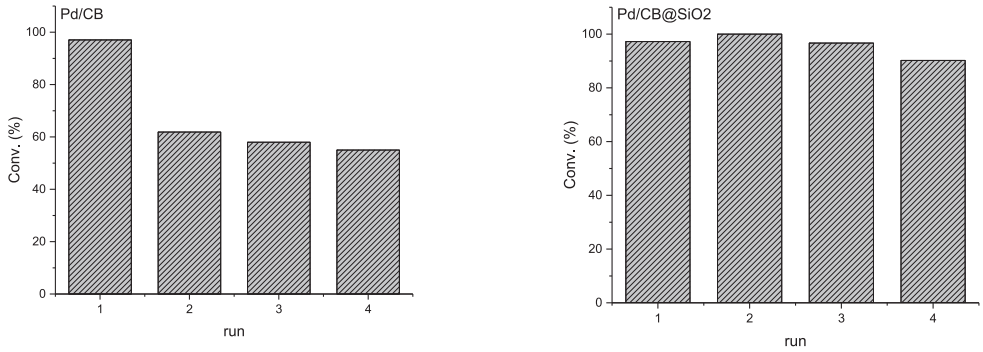

Fig. 4. Benzaldehyde conversion after 3 h of reaction with fresh (run 1) and reused (runs 2–3-4) Pd/CB (left) and Pd/CB@SiO_2 (right) catalysts. Reaction conditions: benzaldehyde 0.3 M in p-xylene, 50 °C, 2 bar H_2, metal/substrate 1:1000.

protected the Pd particles from leaching, maintaining the catalyst activity stable for at least 4 runs. This effect has been explained by considering the physical barrier that the SiO_2 layer can exert on Pd NPs. However, the role of SiO_2 could not be limited to that one, as suggested by the different selectivity showed by the unprotected and protected catalysts.

In previous studies, we demonstrated that NMR relaxometry [3] can be used as a tool for studying the surface interactions between the substrate and the catalyst mediated by the solvent. We therefore applied this technique here in order to disentangle the effect of the SiO_2 layer during the catalytic cycle of benzaldehyde hydrogenation in the presence of Pd/CB and Pd/CB@SiO_2.

We used as substrate both benzaldehyde and benzyl alcohol and measured, as previously reported [3], the T1 relaxation time of each C of benzaldehyde (and benzyl alcohol in the same way) in p-xylene ($T1_{bulk}$) and also after suspending the catalyst in a benzaldehyde (benzyl alcohol)/p-xylene solution ($T1_{ads}$).

The $T1_{bulk}$ and $T1_{ads}$ values and relative calculated ratios obtained for benzaldehyde are reported in Table 1 (related spectra are reported in Fig. S1-6 in the SI).

A $T1_{ads}/T1_{bulk}$ ratio lower than 1 indicates that the molecule has an interaction with the catalyst surface, which is stronger the more the ratio decreases. Looking at the average of the $T1_{ads}/T1_{bulk}$ values obtained for benzaldehyde on Pd/CB or Pd/CB@SiO_2 catalysts (Tab. 2) in the presence of p-xylene as solvent, they are close to 0.9 thus indicating a weak interaction, with a negligible difference when comparing the two catalysts Pd/CB and Pd/CB@SiO_2. However, what can be realized from the individual $T1_{ads}/T1_{bulk}$ values related to each carbon atom of the molecule, is that there is a difference between the C_1 and $C_{2\text{-}5}$ $T1_{ads}/T1_{bulk}$ values on the different catalysts. With the non-protected Pd/CB catalyst, the C_1 $T1_{ads}/T1_{bulk}$ value is lower (0.87) than that obtained in the presence of the protected Pd/CB@SiO_2 catalyst (0.93), suggesting that the Pd/CB catalyst allows a stronger interaction of the carbonyl group of benzaldehyde (C_1) with the catalyst compared to the one obtained in the presence of Pd/CB@SiO_2. Conversely, the C_5 $T1_{ads}/T1_{bulk}$ value is lower (0.82) with the protected Pd/CB@SiO_2 catalyst than that obtained with Pd/CB catalyst (0.94), suggesting that the benzaldehyde could approach differently on the Pd/CB@SiO_2 catalyst, which reduces the C=O interaction in favour of the interaction with the aromatic part of the molecule (Fig. 5).

However, NMR results indicated a different interaction strength between carbon atoms in the molecule (see the T1ads/T1bulk ratio values reported in Table 1).

From here, it is possible to hypothesize a direct approach of the C1 carbonylic carbon of benzaldehyde on the surface of the non-protected Pd/CB catalyst (Fig. 5, left side), which can explain first the faster conversion of benzaldehyde to benzyl alcohol. On the other hand, in the presence of SiO_2 the highest interaction was found to be on C_5, therefore with a leading approach of the aromatic ring (Fig. 5, right side).

The approach of the molecule from the aromatic ring side, in the presence of silica, is supported by some literature reports [31,32]. Very recently, X. Wang [31] reported a study on the interactions in a series of aromatic molecules adsorbed on α-SiO2 surface, using density functional theory (DFT), showing that oxygen-based aromatic molecules interact with such surface because of the formation of weak hydrogen bonds with hydroxylated surface, but also because of the short-range van der Waals interactions of the benzene ring. This latter plays a crucial role in ruling the approach of these molecules on SiO_2-based surfaces. In another work [32], the interaction of limonene and three other cyclic hydrocarbons (cyclohexane, cyclohexene, and benzene) has been investigated on hydroxylated SiO_2, using infrared spectroscopy and ab initio molecular dynamics (AIMD) simulations, and also in this case the experiments

Table 1
Benzaldehyde in *p*-Xylene-*d10*: $T1_{bulk}$ and $T1_{ads}$ resulting from the analysis of the inversion recovery curves from ^{13}C NMR spectra at 400 MHz (C indicates each benzaldehyde carbon atom as labelled in the figure on the left).

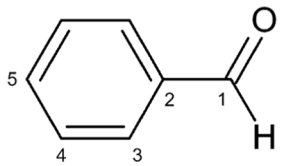

			Pd/CB		Pd/CB@SiO_2	
ppm	**C**	**T1 bulk (s)**	**T1 ads (s)**	**$T1_{ads}/T1_{bulk}$**	**T1 ads (s)**	**$T1_{ads}/T1_{bulk}$**
192	1	16.5	14.5	0.87±0.02	15.3	0.93±0.02
136	2	59.1	63.9	1.00±0.02	54.4	0.92±0.02
134	3	7.88	7.44	0.94±0.02	7.84	0.99±0.02
129	4	11.5	10.9	0.95±0.02	11.1	0.96±0.02
128	5	13.1	12.4	0.94±0.02	10.8	0.82±0.02
				$\bar{x} = 0.94$		$\bar{x} = 0.92$

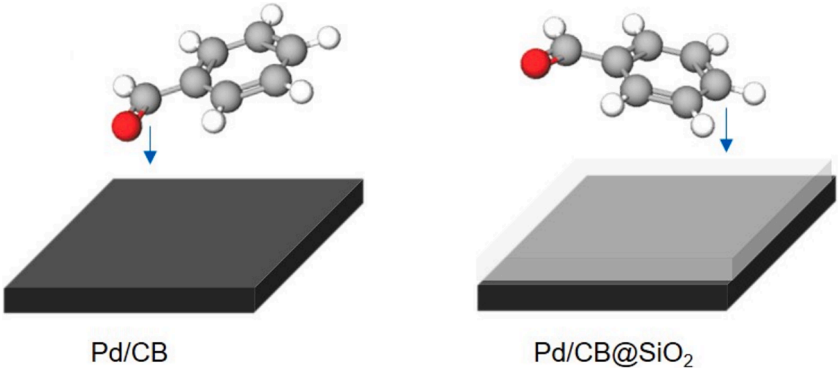

Fig. 5. Benzaldehyde approach to bare Pd/CB (left) and to SiO_2-covered catalyst surface (right).

showed that the interaction between cyclic hydrocarbons and surface hydroxyl groups is ruled by the presence of the aromatic ring.

As the higher interaction of the carbonylic carbon (C_1) on Pd/CB catalyst could be the reason for faster reactivity in converting the aldehyde to the alcohol, it can be supposed that the presence of the SiO_2 layer reduced the interaction of the whole molecule and moved its initial approach more towards the aromatic ring, rather than on the side of the C=O, thus slowing down the aldehyde-alcohol conversion rate.

However, this first consideration is not sufficient to comprehend the different rate of toluene formation using the two different catalysts (Fig. 2).

Indeed, from the reaction profiles (Fig. 2) it is clear that the presence of the SiO_2 layer has an influence also on the benzyl alcohol conversion rate to toluene. This latter, in particular, is strongly reduced by the SiO_2 layer, making the catalyst fully selective to benzyl alcohol if the reaction is stopped at proper reaction time (i.e. 2 h) thus avoiding the formation of toluene (Fig. 2). For this reason, we looked also at the relaxation times of benzyl alcohol, in the presence of p-xylene, comparing the results with Pd/CB and Pd/CB@SiO_2 catalysts (Table 2).

In the case of benzyl alcohol, the average $T1_{ads}/T1_{bulk}$ values are lower than 1 for both catalysts, indicating the presence of an overall interaction even stronger than that shown by benzaldehyde considering the higher $T1_{ads}/T1_{bulk}$ values in the latter case (0.94 vs 0.63 and 0.92 vs 0.83 for Pd/CB and Pd/CB@SiO_2, respectively Tables 1 and 2) but also stronger in the case of Pd/CB than in the case of Pd/CB@SiO_2. In particular, in the case of Pd/CB catalyst (Fig. 6, left side), the overall interaction of benzyl alcohol (C_1 $T1_{ads}/T1_{bulk} = 0.61$, Table 2) can be considered stronger compared to that of benzaldehyde ($T1_{ads}/T1_{bulk} = 0.87$, Table 1). This fact could be a first explanation of the simultaneous formation of toluene with benzyl alcohol that occurred by Pd/CB (see also Fig. 2), where the strong adsorption of benzyl alcohol reduces the interaction of benzaldehyde and allows its immediate conversion to toluene. On the other hand, in the presence of Pd/CB@SiO_2 (Fig. 6, right side), there is still a prime interaction of the aromatic ring instead of the hydroxyl carbon, with $T1_{ads}/T1_{bulk}$ ratio values (Table 2) comparable to those obtained with benzaldehyde (Table 1).

We can thus state that the presence of SiO_2 layer favours the interaction of the aromatic ring thus controlling the way the molecule adsorbs on the active site. In particular, the $T1_{ads}/T1_{bulk}$ values of $C_{4\text{-}5}$ are low enough to ensure the arrival and the interaction of the molecule with the catalyst surface balancing in almost the same way benzaldehyde as well as benzylic alcohol reactions, and most probably in this case two consecutive adsorption/desorption steps can be envisaged for benzaldehyde and benzylic alcohol (see also Fig. 2).

Overall, NMR analyses highlighted that the presence of silica seems to play a role not only in the protection and maintenance of Pd nanoparticle stability, but also in changing and controlling the adsorption mode and strength of the substrates. In particular, the SiO_2 layer provides a significant lower strength of benzyl alcohol than in its absence thus probably allowing the desorption of benzyl alcohol before its consecutive hydrogenolysis. On the contrary, in the case of Pd/CB benzyl alcohol remains strongly adsorbed thus allowing the two steps of the reaction (hydrogenation and hydrogenolysis) to occur consecutively i.e. allowing benzyl alcohol being transformed in toluene without any other desorption/adsorption step. The reason of this different behaviour should be found in both SiO2 functionalities but also in the increasing of surface area. NMR relaxometry provides a useful tool to detect and measure the overall effect of SiO2 layer on Pd/CB which impact both on the stability of the catalyst but also on its selectivity affecting adsorption/desorption of reactant and product of the reaction.

4. Conclusions

A Pd on carbon catalyst (Pd/CB) has been covered by a mesoporous

Table 2
Benzyl alcohol in *p*-Xylene-*d10*: $T1_{bulk}$ and $T1_{ads}$ (in the presence of Pd/CB and Pd/CBCB@SiO_2) resulting from the analysis of the inversion recovery curves from ^{13}C NMR spectra at 400 MHz (C indicates each benzaldehyde carbon atom as labelled in the figure on the left).

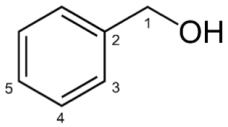

			Pd/CB		Pd/CB@SiO_2	
ppm	**C**	**T1 bulk (s)**	**T1 ads (s)**	**$T1_{ads}/T1_{bulk}$**	**T1 ads (s)**	**$T1_{ads}/T1_{bulk}$**
140.9	1	31.0	19.0	0.61±0.01	30.7	0.99±0.02
128.6	2	45.0	33.2	0.74±0.02	43.3	0.96±0.02
127.7	3	7.59	6.11	0.81±0.02	7.10	0.93±0.02
127.0	4	10.6	3.35	0.32±0.01	8.19	0.77±0.01
65.3	5	9.02	6.02	0.67±0.01	4.28	0.80±0.02
				$\bar{x} = 0.63$		$\bar{x} = 0.83$

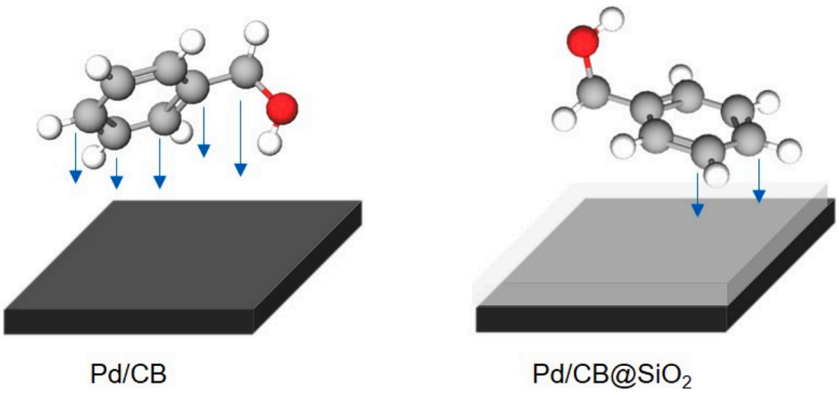

Fig. 6. Benzyl alcohol approach to bare Pd/CB (left) and to Pd/CB@SiO_2 (right).

SiO_2 layer. The synthesis has been carried out for minimizing differences in Pd particle sizes, for studying solely the effect on hydrogenation reaction of the covering layer. Benzaldehyde hydrogenation in p-xylene was used as a test and NMR relaxometry as a tool for studying the different interactions between the catalyst and the reactant/products.

It was found that the two catalysts did not show strong differences in activity although they differed in selectivity. While the Pd/CB catalyst appeared to catalyse at almost the same rate benzaldehyde and benzyl alcohol thus forming toluene at the same rate as benzyl alcohol, the Pd/CB@SiO_2 catalyst allowed to separate the two steps, selectively obtaining both products. Precisely, by Pd/CB@SiO_2 it is possible to maximize the formation of benzyl alcohol in 2 h of reactions, or obtain full conversion of benzyl alcohol to toluene continuing the reaction overtime, being this second step consecutive to the first one. In addition, the SiO_2 layer allowed a better stability of the catalyst compared to bare Pd/CB as highlighted by recycling experiments. ICP as well as TEM analyses confirmed that the advantage of using Pd/CB@SiO_2 catalyst with respect to bare Pd/CB material lies in the blocking of leaching of Pd from the catalyst maintaining almost the same metal dispersion. The latter phenomenon leads to a decline of activity for the bare Pd/CB catalyst after one use.

NMR relaxometry and particularly the evaluation of $T1_{ads}/T1_{bulk}$ values allowed to determine more in detail the active contribution of the SiO_2 layer in modifying the reaction mechanism. Benzaldehyde showed a comparable overall interaction strength with Pd/CB and Pd/CB@SiO_2 catalysts. Nevertheless, Pd/CB interacts more strongly with the carbonyl group while Pd/CB@SiO_2 catalyst presents a higher interaction with the aromatic ring. These differences become more evident when the product, benzyl alcohol, is considered: the strength of interaction with Pd/CB catalyst was very strong, letting us to suppose that benzyl alcohol remained adsorbed when formed and then directly transformed into toluene or, even desorbed, competing with benzaldehyde on the catalyst surface. This in turn leads to a fast transformation of benzyl alcohol to toluene during its formation. The scenario changes when Pd/CB@SiO_2 catalyst is used: in this case benzyl alcohol presents only slightly higher strength of interaction with the catalyst, thus allowing benzyl alcohol to compete with benzaldehyde on the catalyst surface only when benzaldehyde concentration is low. This in turn allows the catalyst to present a very high selectivity to benzylic alcohol for short reaction time or alternatively to toluene by prolonging the reaction time.

CRediT authorship contribution statement

M. Stucchi: Writing – original draft, Methodology, Investigation, Data curation. **A. Engel:** Data curation. **F. Drault:** Data curation. **I. Barlocco:** Writing – review & editing. **A. Villa:** Writing – review & editing, Supervision. **S. Hermans:** Investigation, Data curation. **L. Prati:** Writing – review & editing, Validation, Supervision.

Declaration of competing interest

The authors declare that they have no known competing financial interests or personal relationships that could have appeared to influence the work reported in this paper.

Acknowledgments

The work is supported by an ARC Funding grant (CaScadOS project n° 21/26-117) from Communauté Française de Belgique (Belgium), and by the National Recovery and Resilience Plan (NRRP) and Ministero dell'Università e della Ricerca (MUR) in European Union – NextGenerationEU Project (code PE0000021, Concession Decree No. 1561 of 11.10.2022, project title "Network 4 Energy Sustainable Transition - NEST). The authors also wish to thank the IMERYS GRAPHITE & CARBON firm for generous donation of carbon black.

Appendix A. Supplementary data

Supplementary data to this article can be found online at https://doi.org/10.1016/j.jcat.2025.116195.

Data availability

Data will be made available on request.

References

[1] S. Cattaneo, M. Stucchi, A. Villa, L. Prati, Gold catalysts for the selective oxidation of biomass-derived products, ChemCatChem 11 (2019), https://doi.org/10.1002/cctc.201801243.
[2] S. Capelli, S. Cattaneo, M. Stucchi, B.D. Vandegehuchte, A. Chieregato, A. Villa, L. Prati, The nature of active sites in the Pd/C-catalyzed hydrogenation/hydrodeoxygenation of benzaldehyde, Catalysts 12 (2022), https://doi.org/10.3390/catal12030251.
[3] M. Stucchi, F. Vasile, S. Cattaneo, A. Villa, A. Chieregato, B.D. Vandegehuchte, L. Prati, An Insight into the Role of Reactant Structure Effect in Pd / C Catalysed Aldehyde Hydrogenation, (2022).
[4] S. Cattaneo, S. Capelli, M. Stucchi, F. Bossola, V. Dal Santo, E. Araujo-Lopez, D. I. Sharapa, F. Studt, A. Villa, A. Chieregato, B.D. Vandegehuchte, L. Prati, Discovering the role of substrate in aldehyde hydrogenation, J. Catal. 399 (2021) 162–169, https://doi.org/10.1016/j.jcat.2021.05.012.
[5] M.D. Argyle, C.H. Bartholomew, Heterogeneous catalyst deactivation and regeneration: a review, Catalysts 5 (2015) 145–269, https://doi.org/10.3390/catal5010145.
[6] E. Mine, A. Yamada, Y. Kobayashi, M. Konno, L.M. Liz-Marzán, Direct coating of gold nanoparticles with silica by a seeded polymerization technique, J. Colloid Interface Sci. 264 (2003) 385–390, https://doi.org/10.1016/S0021-9797(03)00422-3.
[7] S. Ghosh, C.P. Jijil, R.N. Devi, In situ encapsulation of ultra small ceria nanoparticles stable at high temperatures in the channels of mesoporous silica, Micropor. Mesopor. Mater. 155 (2012) 215–219, https://doi.org/10.1016/j.micromeso.2012.02.006.

[8] T. Haynes, O. Ersen, V. Dubois, D. Desmecht, K. Nakagawa, S. Hermans, Protecting a Pd/CB catalyst by a mesoporous silica layer, Appl. Catal. B 241 (2019) 196–204, https://doi.org/10.1016/j.apcatb.2018.09.018.
[9] G. Rothenberg, The Basics of Catalysis, in: Catalysis, Concepts and Green Applications, WILEY-VCH, n.d.
[10] Heterogeneous Catalysis, in: Catalysis, 2008: pp. 127–187. DOI: DOI: 10.1002/9783527621866.ch4.
[11] M. Manzoli, Boosting the characterization of heterogeneous catalysts for H2O2 direct synthesis by infrared spectroscopy, Catalysts 9 (2019), https://doi.org/10.3390/catal9010030.
[12] G. Busca, J. Lamotte, J. Ciaude Lavalley, V. Lorenzelli, FT-IR study of the adsorption and transformation of formaldehyde on oxide surfaces, J. Am. Chem. Soc. 109 (1987) 5197–5202, https://doi.org/10.1021/ja00251a025.
[13] B.L. Mojet, S.D. Ebbesen, L. Lefferts, Light at the interface: the potential of attenuated total reflection infrared spectroscopy for understanding heterogeneous catalysis in water, Chem. Soc. Rev. 39 (2010) 4643–4655, https://doi.org/10.1039/C0CS00014K.
[14] S. Campisi, D. Ferri, A. Villa, W. Wang, D. Wang, O. Kröcher, L. Prati, Selectivity control in palladium-catalyzed alcohol oxidation through selective blocking of active sites, J. Phys. Chem. C 120 (2016) 14027–14033, https://doi.org/10.1021/acs.jpcc.6b01549.
[15] M. Stucchi, F. Vasile, S. Cattaneo, A. Villa, A. Chieregato, B.D. Vandegehuchte, L. Prati, An insight into the role of reactant structure effect in Pd/C catalysed aldehyde hydrogenation, Nanomaterials 12 (2022), https://doi.org/10.3390/nano12060908.
[16] M. Stucchi, J.P. Korb, O. Serve, V. Livadaris, B. Vandegehuchte, L. Prati, Low-field 2D NMR relaxometry to disclose the support-substrate interaction and surface dynamics in heterogeneous catalysis: a novel and complementary view to high field NMR relaxometry, J. Catal. 428 (2023) 115168, https://doi.org/10.1016/j.jcat.2023.115168.
[17] P.A. Vecino, Role of adsorption in catalysis : applications of NMR relaxometry, in: 2015.
[18] C. D'Agostino, J. Mitchell, M.D. Mantle, L.F. Gladden, Interpretation of NMR relaxation as a tool for characterising the adsorption strength of liquids inside porous materials, Chem. A Eur. J. 20 (2014) 13009–13015, https://doi.org/10.1002/chem.201403139.
[19] P.A. Vecino, Z. Huang, J. Mitchell, J. McGregor, H. Daly, C. Hardacre, J. M. Thomson, L.F. Gladden, Determining adsorbate configuration on alumina surfaces with 13C nuclear magnetic resonance relaxation time analysis, PCCP 17 (2015) 20830–20839, https://doi.org/10.1039/C5CP02436F.
[20] F. Bloch, Generalized theory of relaxation, Phys. Rev. 105 (1957) 1206–1222, https://doi.org/10.1103/PhysRev.105.1206.
[21] J. Mitchell, T.C. Chandrasekera, M.L. Johns, L.F. Gladden, E.J. Fordham, Nuclear magnetic resonance relaxation and diffusion in the presence of internal gradients: the effect of magnetic field strength, Phys. Rev. E 81 (2010) 26101, https://doi.org/10.1103/PhysRevE.81.026101.
[22] R. Kimmich, Main-Field Gradient NMR Diffusometry, in: R. Kimmich (Ed.), NMR: Tomography, Diffusometry, Relaxometry, Springer Berlin Heidelberg, Berlin, Heidelberg, 1997: pp. 179–190. DOI: 10.1007/978-3-642-60582-6_19.
[23] B.E. Kinn, T.R. Myers, A.M. Allgeier, Surface enhanced nuclear magnetic resonance relaxation mechanisms and their significance in chemical engineering applications, Curr. Opin. Chem. Eng. 24 (2019) 115–121, https://doi.org/10.1016/j.coche.2019.03.010.
[24] M. Stucchi, francesca vasile, stefano cattaneo, alessandro vomeri, A.B. Hungria, L. Prati, Pt-WOx/C catalysts for α, β- unsaturated aldehydes hydrogenation: a NMR study of the effect of the reactant adsorption on activity and selectivity., European J Org Chem n/a (2022). doi: 10.1002/ejoc.202200735.
[25] X.-Q. Xie, S.V. Ranade, A.T. DiBenedetto, A solid state NMR study of polycarbonate oligomer grafted onto the surface of amorphous silica, Polymer (guildf) 40 (1999) 6297–6306, https://doi.org/10.1016/S0032-3861(99)00018-X.
[26] M.V. Popova, Y.S. Tchernyshev, D. Michel, 13C NMR study of the influence of the Aerosil surface charge on the short-chain surfactant adsorption, Colloid Polym. Sci. 285 (2006) 359–363, https://doi.org/10.1007/s00396-006-1565-9.
[27] C. Sievers, A. Onda, R. Olindo, J.A. Lercher, Adsorption and polarization of branched alkanes on H−LaX, J. Phys. Chem. C 111 (2007) 5454–5464, https://doi.org/10.1021/jp067312u.
[28] Y. Hao, C. Pischetola, F. Cárdenas-Lizana, M.A. Keane, Selective liquid phase hydrogenation of benzaldehyde to benzyl alcohol over alumina supported gold, Catal. Lett. 150 (2020) 881–887, https://doi.org/10.1007/s10562-019-02944-y.
[29] T. Haynes, V. Dubois, S. Hermans, Particle size effect in glucose oxidation with Pd/CB catalysts, Appl. Catal. A Gen. 542 (2017) 47–54, https://doi.org/10.1016/j.apcata.2017.05.008.
[30] S. Capelli, S. Cattaneo, M. Stucchi, B.D. Vandegehuchte, A. Chieregato, A. Villa, L. Prati, The nature of active sites in the Pd/C-catalyzed hydrogenation/hydrodeoxygenation of benzaldehyde, Catalysts 12 (2022) 1–12, https://doi.org/10.3390/catal12030251.
[31] X. Wang, Study of physisorption of aromatic molecules on hydroxylated α-SiO2 (001) surface using dispersion-corrected density functional theory, Comput. Theor. Chem. 1220 (2023) 113991, https://doi.org/10.1016/j.comptc.2022.113991.
[32] Y. Fang, P.S.J. Lakey, S. Riahi, A.T. McDonald, M. Shrestha, D.J. Tobias, M. Shiraiwa, V.H. Grassian, A molecular picture of surface interactions of organic compounds on prevalent indoor surfaces: Limonene adsorption on SiO2, Chem. Sci. 10 (2019) 2906–2914, https://doi.org/10.1039/c8sc05560b.